Validation of total water vapor retrieval with an airborne millimeter wave radiometer over Arctic sea ice

Nathalie Selbach,[1] Tim J. Hewison,[2] Georg Heygster,[1] Jungang Miao,[1] Andrew J. McGrath,[2] and Jonathan P. Taylor[2]

Received 11 March 2002; revised 12 July 2002; accepted 13 August 2002; published 30 May 2003.

[1] Measurements of the airborne SEPOR-POLEX campaign in the Arctic in March 2001 were used to validate a total water vapor (TWV) algorithm. This is a modified version of an algorithm developed by *Miao et al.* [2001] using SSM/T2 data in the Antarctic. Data from a passive microwave radiometer with channels at 157, 183 ± 7, 183 ± 3, and 183 ± 1 GHz have been used. Dropsondes were launched from the aircraft during the flights to provide ground truth for the validation of the algorithm. The surface emissivity is assumed to be the same for the frequencies used. In general, there is a good agreement with TWV derived from dropsondes using the 183 GHz data only. This assumption leads to systematic errors in the estimation of TWV if the 157 GHz data are used in combination with measurements at 183 GHz. The high surface emissivity in regions of new ice is shown to lead to errors as a result of the strong influence of the surface. The difference in emissivity between 157 GHz and 183 GHz is larger over open water than over the sea ice, and therefore the error in TWV using the lower frequencies is larger in these regions. *INDEX TERMS:* 3349 Meteorology and Atmospheric Dynamics: Polar meteorology; 3360 Meteorology and Atmospheric Dynamics: Remote sensing; 3394 Meteorology and Atmospheric Dynamics: Instruments and techniques; 0368 Atmospheric Composition and Structure: Troposphere-constituent transport and chemistry; 1610 Global Change: Atmosphere (0315, 0325); *KEYWORDS:* water vapor, microwave radiometry, remote sensing, polar atmosphere

Citation: Selbach, N., T. J. Hewison, G. Heygster, J. Miao, A. J. McGrath, and J. P. Taylor, Validation of total water vapor retrieval with an airborne millimeter wave radiometer over Arctic sea ice, *Radio Sci., 38*(4), 8061, doi:10.1029/2002RS002669, 2003.

1. Introduction

[2] Recent studies in atmospheric and oceanic circulation have shown that polar regions play an important role in the global climate variability and change. Therefore there is an increasing interest in the research of these regions [*Bromwich*, 1997]. However, due to the remoteness of these areas and their demanding climate, direct measurements of many useful geophysical parameters in polar regions are very sparse [*King and Turner*, 1997]. Satellite microwave radiometry, due to its good spatial and temporal coverage, potentially provides a valuable tool for global observation of atmospheric parameters like columnar water vapor and cloud liquid water. But difficulties arise from the large and highly changeable surface emissivity at microwave bands from the ice/snow covered surface together with the very low water vapor burden in polar regions.

[3] By making use of the specific features of the Special Sensor Microwave/Temperature-2 (SSM/T2) instrument onboard the DMSP satellites, a method was proposed recently for the measurement of total water vapor (TWV) under complex ground surface conditions [*Miao*, 1998]. This method was originally developed for Antarctic conditions and has shown its usefulness for Antarctic meteorological and climatological studies [*Miao et al.*, 1997, 2001]. More recently, *Wang et al.* [2001] showed that this method could be extended to sea ice covered Arctic regions. *Wang et al.* [2001] discussed the problem of difference in surface emissivities at the used channels. An iterative method was proposed to solve this problem assuming a linear function with frequency for the surface emissivity within the narrow range of the used channels. However, the results of *Wang et al.* [2001] were limited to TWV values around 5 kg/m^2, which is close to the limitation of the capability of the used channels. In addition, a comparison with

[1]Institute of Environmental Physics, University of Bremen, Bremen, Germany.
[2]Met Office, Farnborough, UK.

0048-6604/03/2002RS002669$11.00

Table 1. Summary of SSM/T2 and AMSU-B Channel Parameters

Channel Number	Center Frequency, GHz	IF Bandwidth, GHz	Beam Width (FWHM)	Calibration Accuracy, K
		SSM/T2		
4	91.665 ± 1.250	1.5	6.0°	0.6
5	150.00 ± 1.25	1.5	3.7°	0.6
2	183.310 ± 1.000	0.5	3.0°	0.8
1	183.310 ± 3.000	1.0	3.0°	0.6
3	183.310 ± 7.000	1.5	3.0°	0.6
		AMSU-B		
16	89.0 ± 0.9	1.0	1.1°	0.37
17	150.00 ± 0.9	1.0	1.1°	0.84
18	183.310 ± 1.000	0.5	1.1°	1.06
19	183.310 ± 3.000	1.0	1.1°	0.70
20	183.310 ± 7.000	2.0	1.1°	0.60

coincident radiosonde measurements was only done in two cases.

[4] To further validate the TWV retrievals from microwave radiometry in the Arctic, a campaign was carried out during March 2001. This will be described in the following section. Beside the validation of water vapor retrievals over a range of humidities, the aim of this campaign was to improve the use of satellite data in the marginal ice zone and over first and multiyear ice. These areas have been shown to play a key role in dynamical developments, and represent a currently data sparse area.

2. Data Set

[5] The data set consists of measurements recorded during the airborne SEPOR-POLEX (Surface Emissivities in Polar Regions-Polar Experiment) campaign from 8 to 29 March, 2001.

2.1. Instrumentation

[6] The key instrument for this experiment operated on the Met Office C-130 research aircraft was the passive microwave radiometer MARSS (Microwave Airborne Radiometer Scanning System) with frequencies close to those of SSM/T2 and AMSU-B (Advanced Microwave Sounding Unit-B). Table 1 shows the characteristics of these sensors [*Aerojet GenCorp*, 1990; *Saunders et al.*, 1995]. MARSS is a total power radiometer with a 3 s along-track scan, including various downward and upward views and two onboard black body calibration targets. Further detail is given by *McGrath and Hewison* [2001]. Table 2 summarizes the performance of the radiometer during the campaign. A broad range of meteorological and navigational instruments are operated on the aircraft. These include measurements of air temperature, humidity, pressure and wind velocity, GPS position, radar altitude and surface temperature from a thermal infrared radiometer. The aircraft was also fitted with downward and forward facing video cameras to identify surface conditions.

[7] Atmospheric profiles of pressure, temperature, humidity and wind are available from dropsondes. The RD93 dropsondes [*Hock and Franklin*, 1999] are fitted with Vaisala RS90 humidity sensors. Table 3 summarizes the main characteristics of the dropsondes used during the campaign. The dropsondes were found to have a dry bias of about 8% in mass mixing ratio [*Vance*, 2001], which was corrected in this study. The TWV is calculated from 52 dropsonde profiles which are used for the validation of the TWV retrieval.

2.2. Flights

[8] Five flights of up to 10 hours duration were performed over various ice types in the Arctic including new, glacier, first and multiyear ice between 8 and 29

Table 2. Summary of MARSS Channel Parameters during SEPOR-POLEX

Channel Number	Center Frequency, GHz	IF Bandwidth, GHz	Beam Width (FWHM)	Calibration Accuracy, K
16	88.992 ± 1.1	0.6	11.8°	0.9
17	157.075 ± 2.6	2.2	11.0°	1.1
18	183.248 ± 1.0	0.5	6.2°	1.0
19	183.248 ± 3.0	1.0	6.2°	0.9
20	183.248 ± 7.0	2.0	6.2°	0.8

Table 3. Dropsonde Parameters

Parameter	Operating Range	Accuracy Repeatability	Accuracy Uncertainty in Soundings	Resolution	Time Constant
Pressure, hPa	100–1080	0.4	1.5	0.1	<0.01 s
Temperature, °C	−90 to 40	0.1	0.5	0.1	2.5 s (at 20°C) 3.7 s (at −40°C)
Humidity, %	0–100	2	5	1	0.1 s (at −20°C) 10 s (at −40°C)
Horizontal Wind, m s^{-1}	0–200	0.5		0.1	

March 2001. Figure 1 shows a plot of the five flight tracks with an underlying ice concentration on 23 March 2001. The ice concentration was derived from Special Sensor Microwave/Imager (SSM/I) 85 GHz data [*Kaleschke et al.*, 2001].

[9] Two flights, marked D and E in Figure 1, concentrated on measurements of the marginal ice zone to collect data over a range of varying ice concentrations and different forms of young and new ice as well as first year ice. The remaining three flights (A, B and C) consisted of long runs up to 85°N and different longitudes (30°E, 0°E, 30°W, respectively).

[10] There was a northerly or north-easterly surface flow over the ice during all flights. This resulted in mainly clear skies over the ice but a rapid cloud development over open water in the marginal ice zone. TWV derived from dropsonde data ranged from approximately 1–3 kg/m^2.

[11] Each flight consisted of a long low level run (approximately 170 m to 1200 m above sea level) over the ice to measure its emissivity, a profile ascent and a run back to the base (Tromsø, 69°41' N, 18°55' E) over the same track at high level (about 9 km above sea level), releasing drop sondes to provide ground truth for the retrieval at approximately 100 km intervals.

3. Retrieval Algorithm

[12] Miao's original algorithm was developed for the SSM/T2 instrument, which has channels close to those of MARSS [*Miao*, 1998]. This exploited the fact that the surface emissivities are expected to be identical for the three channels centered on the 183.31 GHz water vapor absorption line. Using a ratio of brightness temperature (T_b) differences, one obtains an expression independent of surface conditions. The logarithm of this ratio is almost linearly proportional to the TWV weighted with sec θ where θ is the angle of the instrument's view away from nadir. The total water vapor is determined using the following expression

$$\eta = \frac{T_b(183 \pm 7) - T_b(183 \pm 3) - Y_0}{T_b(183 \pm 3) - T_b(183 \pm 1) - X_0} \qquad (1)$$

where (X_0, Y_0) are empirical parameters described below. The logarithm of η linearly depends on the TWV weighted with the secant of the incidence angle θ:

$$TWV \cdot \sec(\theta) = C_0 + C_1 \cdot \ln \eta \qquad (2)$$

However, the application of this algorithm is limited to TWV values below 1.5 kg/m^2 due to saturation effects of the 183 ± 1 GHz channel. For higher values one is forced to include measurements from channels less sensitive to atmospheric water vapor. *Miao et al.* [2001] used the 150 GHz channels for TWV values of up to 6 kg/m^2.

[13] For this study, the channel at 157 GHz was used instead. In order to obtain an algorithm suitable to be used with this channel combination new coefficients (C_0, C_1, X_0, Y_0) were developed. The radiative transfer model MWMOD [*Fuhrhop et al.*, 1998] was used to calculate brightness temperatures for the channels mentioned. For these calculations the absorption coefficients of the *Liebe et al.* [1993] model were used. The model was run with surface emissivities ranging from 0.65-0.94 for 400 arctic profiles of the NESDIS data set. The surface was assumed to be at 1013 hPa at a temperature equal to the temperature at the lowest level of the atmospheric profile. The model is run for both sidebands of the three channels at 183 GHz to account for the asymmetry of the atmospheric absorption in dry atmospheres. Ignoring this feature could lead to errors in the retrieval of TWV [*Wang et al.*, 2001].

[14] To calculate the point (X_0, Y_0) used in (1), the calculated brightness temperature differences are divided into groups of constant TWV with changing surface emissivity. Linear regression is applied for each of these groups. Extending these lines to higher surface emissivities reveals that these lines do not intersect at a common point. Instead, the point (X_0, Y_0) with the minimum distance for all lines is used. Figure 2 shows a plot of brightness temperature differences and the focal point (X_0, Y_0) for the 157 GHz channel and the two wider 183 GHz channels.

[15] Depending on the TWV range two different groups of brightness temperatures are used to determine

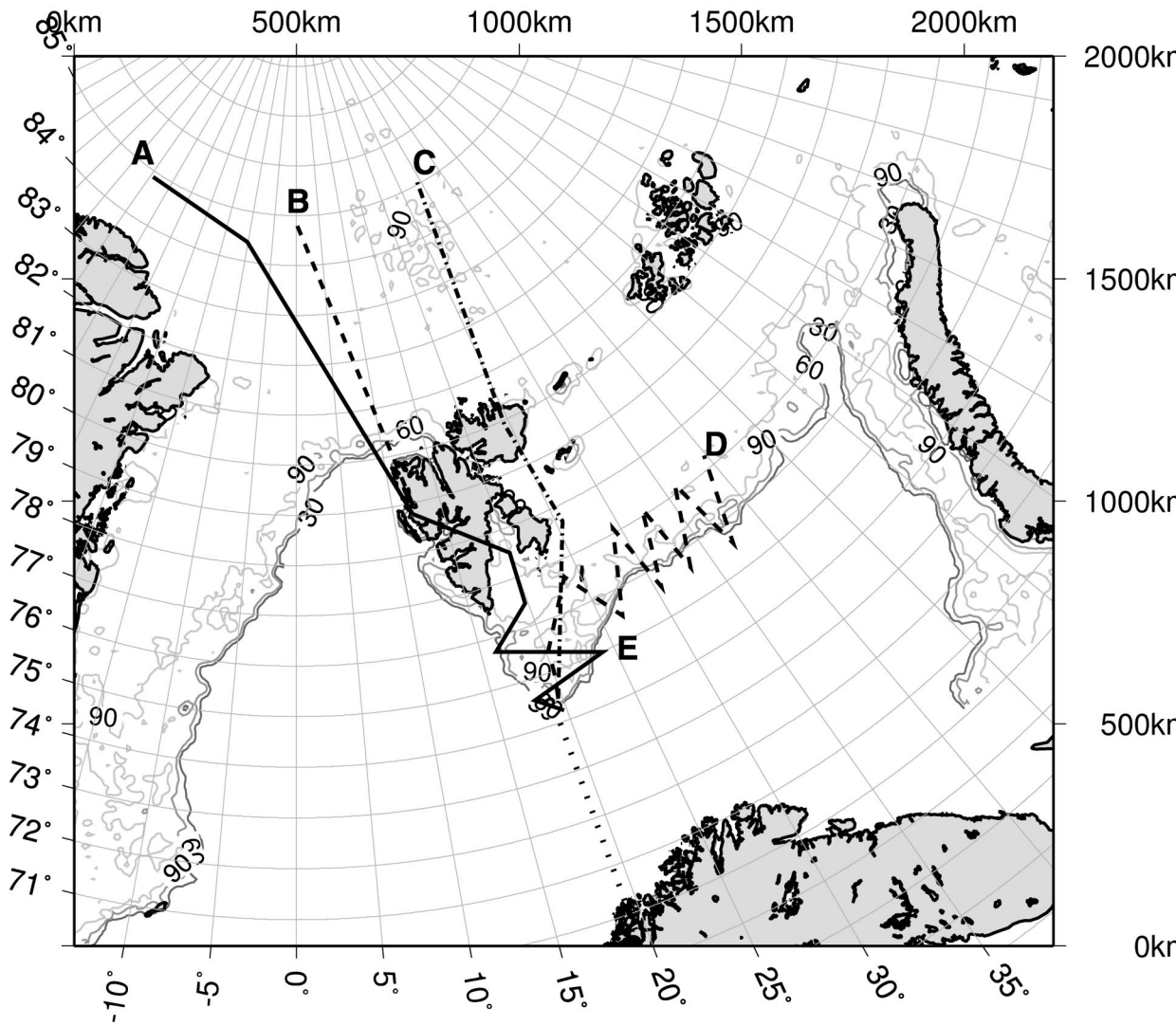

Figure 1. Flight tracks superimposed on the sea ice concentration derived from SSM/I 85 GHz data from 23 March 2001. Isolines of the ice concentration (30%, 60%, and 90%) are also given.

TWV. For TWV < 2 kg/m^2 the three channels at 183 GHz are used, while for the range of 2 kg/m^2 $<$ TWV < 6 kg/m^2 the 157 GHz and the two wider 183 GHz channels are used. The coefficients (C_0, C_1, X_0, Y_0) for both algorithms used in this study are given in Table 4.

[16] The algorithm was developed assuming cloud-free conditions. Nevertheless, *Miao et al.* [2001] have shown that liquid water clouds only have a small effect on the retrieval while ice clouds may result in an underestimation of TWV.

4. Result

4.1. Brightness Temperatures

[17] Figure 3 (top) shows a typical time series of brightness temperatures from 9 km altitude for the flight marked A in Figure 1 to 85° N, 30° W. In general, a decrease in brightness temperature (T_b) due to lower surface temperatures is found for all channels of MARSS. The aircraft's thermal infrared radiometer measured −46° C at 85° N.

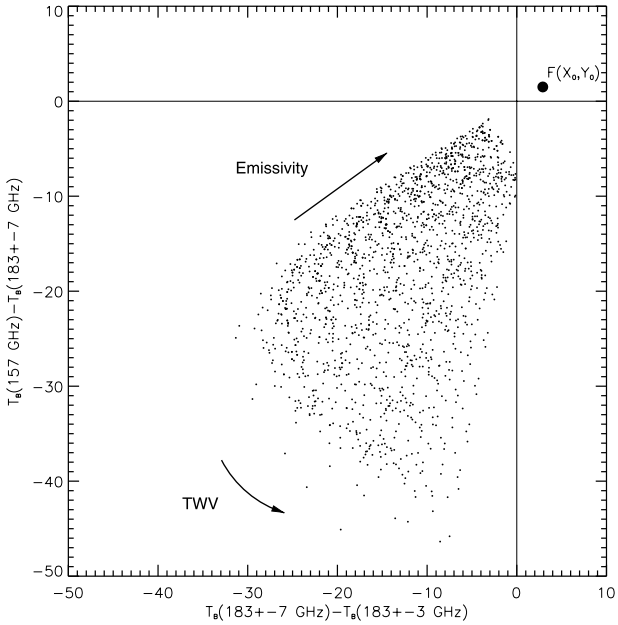

Figure 2. Brightness temperature differences and focal point for 157 GHz and the two wider 183 GHz frequencies.

[18] According to the ice type analysis from NASA TEAM [*Cavalieri et al.*, 1984] multiyear ice was expected for the last part of this low level run. A significant change in T_b was observed for the channels at 89 GHz and 157 GHz, while there was less change in the signal of the channels at 183 GHz. First year and multiyear ice can be distinguished from the data at high level as well (Figure 3). The brightness temperature at 89 GHz is lower than at 157 GHz over the region of multiyear ice (approximately 13:30–13:50 UTC).

[19] Extensive fields of new ice and nilas (e.g., at about 14:05 UTC and 14:22 UTC) within consolidated pack ice (first year ice) show much higher brightness temperatures compared to the signal of first year ice. This is due to the high surface emissivity of this ice type. *Hewison and English* [1999] measured the emissivity of new ice in the Baltic Sea at 157 GHz to be 0.915 at nadir both with and without snow cover. Additionally, open water can clearly be distinguished from sea ice at 89 GHz and 157 GHz (15:18 to 15:30 UTC). The brightness temperatures here show less variation than over ice, especially when compared to the region near the ice edge with changing ice types and ice concentration. In the milder conditions found over open water, the atmosphere becomes practically opaque to the 183 ± 1 GHz channel. This channel then only detects emission from water vapor at colder, upper levels and becomes insensitive to changes at low level.

Table 4. Coefficients of TWV Algorithm

Channels	C_0	C_1	X_0	Y_0
183 GHz only	0.420	0.966	3.528	2.632
157 GHz and 183 GHz	1.580	2.132	2.895	1.521

4.2. Total Water Vapor

[20] Figure 3 (bottom) shows a time series of derived TWV for the same flight as discussed above. The TWV derived from the dropsonde data of this flight ranges from 1.5 kg/m^2 to 2.8 kg/m^2.

[21] The algorithm using the three channels at 183 GHz is in good agreement with the dropsonde data at these low TWV burdens. Problems occur in the case of saturation of the most sensitive channel, for example in the region of open water at 15:30 UTC, where the algorithm fails. For this reason, values with $T_b(183 \pm 3) > T_b(183 \pm 1)$ have to be excluded from the analysis. These TWV values are shown in Figure 3 (bottom), too, to demonstrate the effect of saturation of the 183 ± 1 GHz channel.

[22] Due to the emissivity difference between the channels at 183 GHz and the lower frequency at 157 GHz, the algorithm including the 157 GHz channel shows a systematic positive bias over first year ice. The surface emissivity at 157 GHz is lower than for the 183 GHz channels. Therefore the absolute brightness temperature difference is higher than expected, as the emissivities were assumed to be independent of frequency. This leads to an overestimation of TWV. The difference in surface emissivity is higher for open water than for first-year ice resulting in larger errors in the retrieval (Figure 3, bottom). Nevertheless, Figure 3 (bottom) shows that the algorithm including the lower frequencies follows the principal behavior of the TWV derived from dropsondes.

[23] An increase in retrieved TWV can be seen applying both channel combinations (Figure 3, bottom) in regions of new ice and nilas. Further analysis of the available data, for example a comparison with data from the nearest dropsonde, shows that this is not a real effect. This observed phenomenon can be explained by the surface emissivity of this ice type (see section 4.1). A high surface emissivity results in small brightness temperature differences (Figure 2). Therefore small changes in these differences result in larger changes in TWV. The change in the signal over new ice seems to be mainly influenced by the high surface emissivity itself at the channels used for the retrieval of TWV.

[24] Figure 4 shows a scatterplot of TWV estimated from the dropsonde data and derived from the two different channel combinations for all dropsondes launched during the campaign. The error of the TWV derived from dropsonde data is estimated to be 10%,

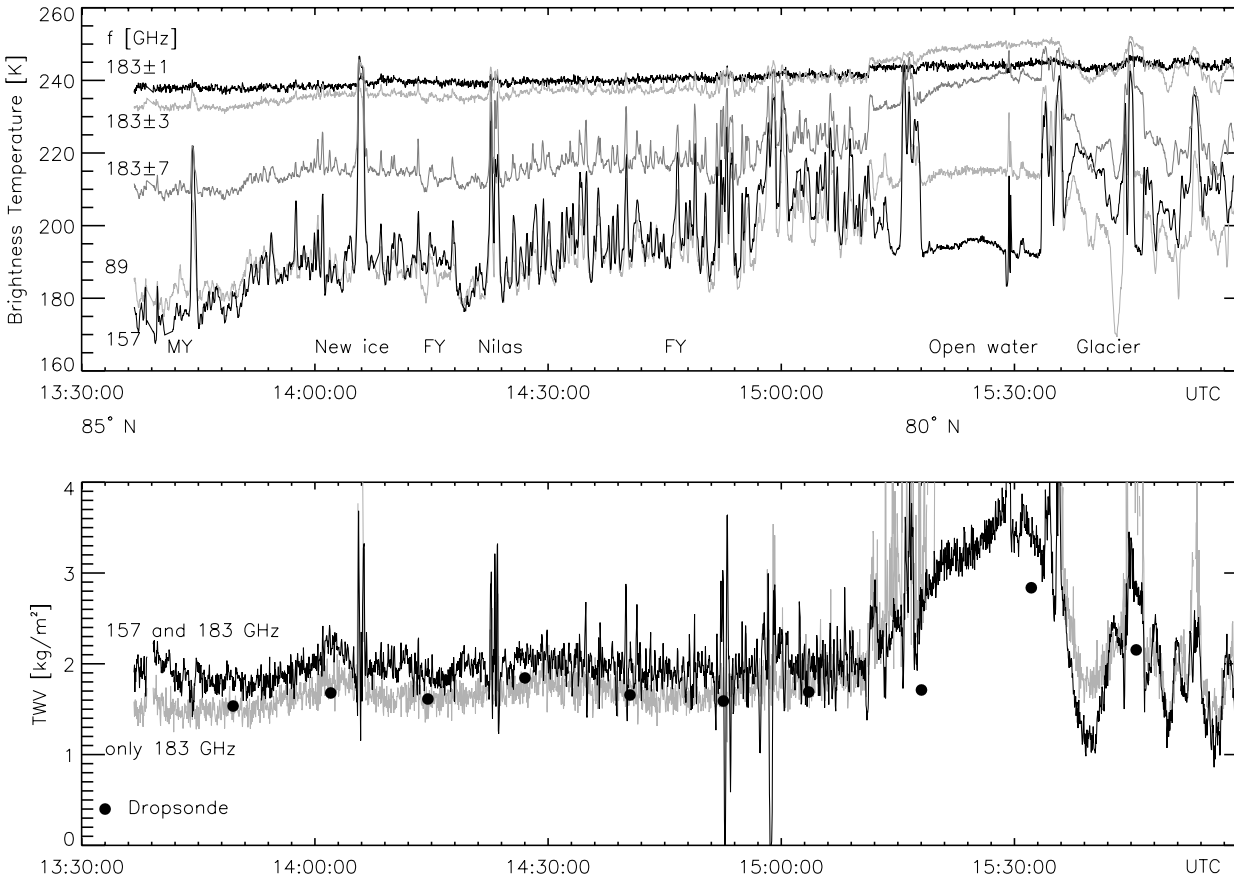

Figure 3. Time series of (top) nadir brightness temperatures from 9 km altitude and (bottom) derived TWV for the flight marked A in Figure 1.

resulting from the uncertainty of the measurements. For the algorithm using the 183 GHz channels only values are shown for which the TWV derived from dropsonde is lower than 2 kg/m^2. The value plotted for the TWV derived from microwave radiometer data is a mean value for a 30 s sample at the time of launch of the dropsonde and one standard deviation as error bars.

[25] The TWV derived from only the 183 GHz channels shows excellent agreement with the dropsondes. The rms error is 0.11 kg/m^2 (approximately 7%) and the mean bias of 0.07 kg/m^2 is better than the quoted accuracy of the dropsondes. When the 157 GHz channel is included in the algorithm, its rms error increases to 0.44 kg/m^2 (about 22%) and the mean bias increases to 0.55 kg/m^2, which is significantly higher than the uncertainty in the dropsondes. This demonstrates that a systematic error was introduced by the assumption of frequency independent emissivity.

5. Conclusion

[26] This study confirms the method proposed by *Miao* [1998] for retrieving TWV over complex ground surface conditions by using measurements close to the 183 GHz water vapor line. At the same time it demonstrates the problem that the difference in surface emissivity leads to errors in deriving TWV using the channel combination including measurements at 157 GHz, as already pointed out by *Wang et al.* [2001]. Taking the frequency dependence of the surface emissivity into account is important for the improvement of the retrieval of TWV in polar regions. This will follow an examination of emissivity from low-level runs of the SEPOR-POLEX experiment. *Wang et al.* [2001] used additional measurements at 220 GHz to develop a TWV algorithm including a correction for the difference in surface emissivity in the frequency range between

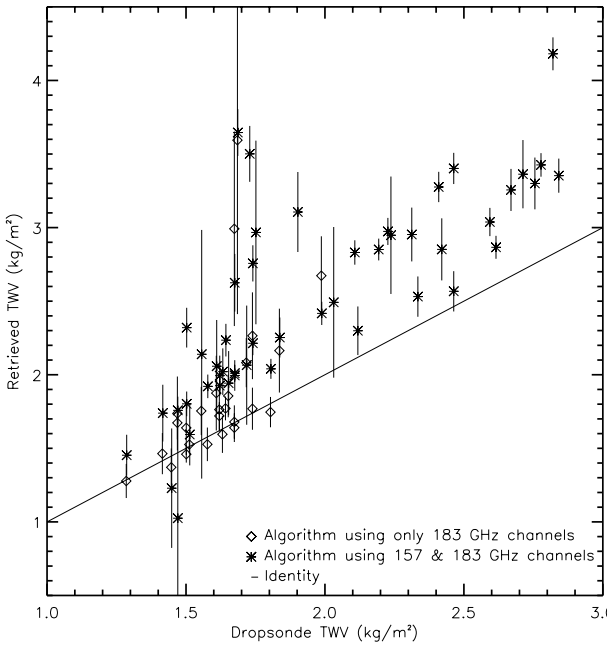

Figure 4. TWV calculated from dropsonde and derived from microwave radiometer data for all SEPOR-POLEX flights.

150 GHz and 220 GHz. Measurements at this high frequency are not available for this study, or for application to current satellite sensors. It is therefore important to develop another method to parameterize the change in surface emissivity with frequency.

[27] The algorithm developed by *Miao et al.* [2001] is limited to TWV values less than 6 kg/m^2. This range is not sufficient to cover the ice and snow covered polar regions. An extension of the range of the TWV algorithm by including the 89 GHz channel with a lower sensitivity to water vapor may be possible. This will require a further consideration of Arctic surface emissivity spectra. Measurements at this frequency and also some data at 24 and 50 GHz to derive this parameter are available from this campaign.

[28] These studies have shown the potential of deriving TWV from millimeter wave radiometry over ice surfaces in both the Antarctic, and now the Arctic. This algorithm will also be evaluated over snow covered land surfaces with low TWV.

[29] **Acknowledgments.** SEPOR was funded under the Framework Programme V—Improving the Human Research Potential and Socio Economic Knowledge Base under the Transnational Access to major Research Infrastructures from the CAATER programme, contract HPRI-CT-1999-00095. The authors wish to thank the staff of the Norwegian Meteorological Institute (DNMI) for their support and hospitality in Tromsø. The authors would like to acknowledge the dedication and support of the aircraft's ground and air crew and the scientists and technicians of the Meteorological Research Flight. We are also grateful to MultiNet AS for the provided Internet service. We thank three anonymous reviewers for their helpful comments.

References

Aerojet GenCorp, System summary report for the SSM/T2 water vapor profiling sensor hardware segment, report, Dep. of the Air Force, Azusa, Calif., 1990.

Bromwich, D. H., Introduction to special section: Synoptic and Mesoscale Weather System in the Polar Regions, *J. Geophys. Res.*, *102*, 13,727–13,729, 1997.

Cavalieri, D. J., P. Gloersen, and W. J. Campbell, Determination of sea ice parameters with the NIMBUS 7 SMMR, *J. Geophys. Res.*, *89*, 5355–5369, 1984.

Fuhrhop, R., T. C. Grenfell, G. Heygster, K.-P. Johnsen, P. Schlüssel, M. Schrader, and C. Simmer, A combined radiative transfer model for sea ice, open water, and atmosphere, *Radio Sci.*, *33*, 303–316, 1998.

Hewison, T. J., and S. J. English, Airborne retrievals of snow and ice surface emissivity at millimeter wavelengths, *IEEE Trans. Geosci. Remote Sens.*, *37*, 1871–1879, 1999.

Hock, T. F., and J. L. Franklin, The NCAR GPS dropwindsonde, *Bull. Am. Meteorol. Soc.*, *80*, 407–420, 1999.

Kaleschke, L., C. Lüpkes, T. Vihma, J. Haarpaintner, A. Bochert, J. Hartmann, and G. Heygster, SSM/I sea ice remote sensing for mesoscale ocean-atmosphere interaction analysis, *Can. J. Remote Sens.*, *27*, 526–537, 2001.

King, J. C., and J. Turner, *Antarctic Meteorology and Climatology*, 409 pp., Cambridge Univ. Press, New York, 1997.

Liebe, H. J., G. A. Hufford, and M. G. Cotton, Propagation modeling of moist air and suspended water/ice particles at frequencies below 1000 GHz, paper presented at AGARD 52nd Specialists Meeting of the Electromagnetic Wave Propagation Panel, Advisory Group for Aerospace Res. and Development, Palma de Mallorca, Spain, 17–21 May 1993.

McGrath, A., and T. Hewison, Measuring the accuracy of MARSS—An airborne microwave radiometer, *J. Atmos. Oceanic Technol.*, *18*, 2003–2012, 2001.

Miao, J., *Retrieval of atmospheric water vapor content in polar regions using spaceborne microwave radiometry*, *Rep. Polar Res. 289*, 109 pp., Alfred Wegener Inst. for Polar and Mar. Res., Bremerhaven, Germany, 1998.

Miao, J., N. Schlueter, and G. Heygster, Retrieval of total water vapor in polar regions using SSM/T2 channels, paper presented at 1997 IEEE International Geoscience and Remote Sensing Symposium, Inst. of Electrical and Electronics Eng., Singapore, 1997.

Miao, J., K. Kunzi, G. Heygster, T. A. Lachlan-Cope, and J. Turner, Atmospheric water vapor over antarctica derived from special sensor microwave/temperature: 2. Data, *J. Geophys. Res.*, *106*, 10,187–10,203, 2001.

Saunders, R. W., T. J. Hewison, S. J. Stringer, and N. C. Atkinson, The radiometric characterization of AMSU-B, *IEEE Trans. Microwave Theory Technol.*, *43*, 760–771, 1995.

Vance, A., M.O.T.H: Comparison of in-situ humidity data, *MRF Tech. Note 32*, Met Off., Farnborough, UK, 2001.

Wang, J. R., P. E. Racette, and M. E. Triesky, Retrieval of precipitable water vapor by the millimeter-wave imaging radiometer on the arctic region during FIRE-ACE, *IEEE Trans. Geosci. Remote Sens.*, *39*, 595–605, 2001.

T. J. Hewison, A. J. McGrath, and J. P. Taylor, Met Office, Y70, Cody Technology Park, Ively Road, Farnborough Hampshire GU14 0LX, UK. (tim.hewison@metoffice.com)

G. Heygster, J. Miao, and N. Selbach, Institute of Environmental Physics, University of Bremen, P.O. Box 330440, 28334 Bremen, Germany. (nselbach@uni-bremen.de)